1-1-2013

Equation of State and Isentropic Releasem of Aluminum Foam and Fluoropolymer Composites

John Borg
Marquette University, john.borg@marquette.edu

Warren R. Maines
Air Force Research Laboratory

Mike Nixon
Air Force Research Laboratory

Lalit Chhabildas
Air Force Research Laboratory

Published version. *Procedia Engineering*, Vol. 58 (2013): 299-308. DOI.

Available online at www.sciencedirect.com

SciVerse ScienceDirect

Procedia Engineering 58 (2013) 299 – 308

Procedia Engineering

www.elsevier.com/locate/procedia

The 12th Hypervelocity Impact Symposium

Equation of State and Isentropic Releasem of Aluminum Foam and Fluoropolymer Composites

John P. Borg[a]*, Warren R. Maines[b], Mike Nixon[b] and Lalit Chhabildas[b]

[a]*Marquette University, 1515 W. Wisconsin, Milwaukee, WI, 53233, USA*
[b]*Air Force Research Laboratory, Damage Mechanisms Branch, Eglin AFB, FL 32542*

Abstract

There is considerable interest in developing a better understanding of the dynamic behavior of heterogeneous materials. This study investigates and compares the dynamic response of 20 and 47% dense aluminum foam systems with and without a polytetrafluoroethylene (PTFE or Teflon) fill. Experiments on 47% foam were conduced in a 60 mm bore gun in a reverse ballistic configuration at velocities ranging from 350 m/s to 2.5 km/s. The particle velocity of the backside of the anvil was monitored with a VISAR system. Mesoscale simulations are in good agreement with the available experimental data. Both the experimental and simulated data are in good agreement with an analytic release isentrope when released from Hugoniot stress levels less than 5 GPa. However there is significant deviation from the analytic isentrope as the Hugoniot stress level is increased.

Selection and peer-review under responsibility of the Hypervelocity Impact Society

Keywords: Aluminum Foam, Hugoniot, Isentrope, CTH, mesoscale simulations

1. Background

Many engineering problems involve systems of heterogeneous materials experiencing rapid dynamic loading; examples include reactive materials, penetration as well as blast and impact loading. The dynamic behavior of heterogeneous materials, including granular, foam or composite systems, is fundamentally a multi-scale problem involving interactions between multiple material constituents, including either a void space (porosity) or filler (binder). Open cell foams, as opposed to closed cell foams, contain joined pores that form an interconnected pore network. As a result, open cell foams can be completely filled with a fluid which when cured can serve as filler. Systems constructed in this way could take advantage of the mixed constitutive components including mixed strength, reactivity and impedance differences. The result could be made-to-order engineered structures that perform a given task when dynamically loaded. This work is focused on developing a better understanding of the dynamic behavior of open cell structured aluminum foam systems with and without a filler material at two different mix ratios.

The behavior of the heterogeneous structures at small scale can affect the behavior at large scale. When a large volume of the structure is considered, the bulk scale, which might include thousands of pores, the material can behave, and be modeled, somewhat like a homogeneous continuum. Which is to say, the material can be assigned volume-averaged properties. The dynamic loading then results in a homogeneous stress state behind the compaction wave. However as the characteristic dimension of a representative volume is reduced, the dominant phenomenological behavior within this volume varies, as does the thermodynamic state of the material. At still smaller scales, on the order of a pore, the solid material

* Corresponding author. Tel.: +1-414-288-7519; fax: +1-414-288-7790.
E-mail address: john.borg@mu.edu.

Selection and peer-review under responsibility of the Hypervelocity Impact Society
doi:10.1016/j.proeng.2013.05.034

experiences vastly differing stress states compared to the pore space material. Interactions at the scale of a filled pore are dominated by rapid shock and release processes that result in local anisotropic states. The result is a complicated multi-scale stress field where portions of the solid structure can carry nearly the entire load while some structures carry nearly no load. At yet smaller scales, on the order of the foam structure, the material interconnectivity and contact determine the transmission of stress through the solid structure network. At even smaller scales (those less than the foam structure itself) the non-isotropic material rheology behavior, such as yield and deformation, plasticity and twinning, establish the dominant phenomenological behavior characteristics. Phenomenology at all of these scales feeds back to the bulk scale and ultimately dictate the response of the overall bulk system. However it remains unclear as to which mechanisms dominate and which, if any, might therefore be neglected. The simulations presented here resolve the dynamic compaction behavior from the bulk scale to the structure of the foam. At the scale of the foam structure and smaller the material is treated as a homogenous continuum solid. Thus the simulations resolve the complicated shock and release interactions between the foam and pore structures as well as the evolution of the pores. Thus the term *meso*-scale, which means middle scale, is used to describe the simulations presented here in that the interaction between the bulk and grain scale are resolved.

The work presented here focuses on filled and unfilled aluminum systems. The dynamic loading of aluminum foam systems has been the focus of several dynamic experiments [1-5] as well as mesoscale simulations [6,7]. The shock and release of these porous structures has been characterized by experiments and is in good agreement with theoretical predictions in the range of the experimental results. The current work deviates from these investigations in two ways. First the initial foam density is much lower than the previously reported work. Second, the systems investigated here include both Teflon filled and unfilled pore networks

2. Introduction

In this work we perform two and three-dimensional mesoscale simulations of aluminum-Teflon systems subjected to a plane strain shock and release process. The 47% dense foam is investigated both with and without the Teflon filler whereas the 20% dense aluminum foam is only investigated as a Teflon filled system. We proceed by initially investigating the unfilled 47% aluminum foam and comparing the results to experiment. We follow this by investigating a Teflon filled 47% aluminum foam system and then finally adjusting the percent mix of constituents to 20% aluminum foam with the Teflon fill. By taking a progression of steps we build confidence in our modeling while working towards a completely predictive capability.

Dynamic testing at high strain rates was investigated in a reverse ballistics plane strain configuration where the impact velocities varied from 0.4 to 2.2 km/s. This is referred to as a reverse ballistics configuration because the material of interest is the flyer plate and impacts a well-characterized witness plate. Figure 1a presents a schematic of the shock and release process in x-t space, where shocks are drawn as solid arrows and release processes drawn as dashed arrows. The result is a left-traveling shock launched into the material followed by a series of release waves emanating from the witness plate. A variety of witness plates were used in the experiments in order to vary the initial Hugoniot state achieved. The corresponding process is drawn in pressure-particle velocity space in Figure 1b. The reverse ballistic configuration allows one to measure both the Hugoniot state and the isentropic release path through multiple reverberations. Since the particle velocity of the backside of the witness plate is monitored with a laser interferometer system, i.e. a VISAR, the even number states (u_2, u_4, u_6, ...) can be measured. By knowing these velocity states and using the impedance matching technique illustrated in Figure 1b, the shock and release behavior in the foam can be inferred from the VISAR record.

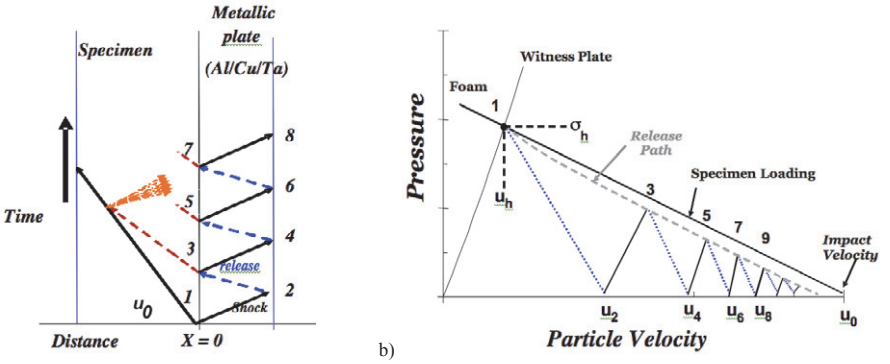

Figure 1: Wave interactions in a reverse ballistics configuration.

3. Experimental and Computational Setup

The ERG Aerospace aluminum foam was modeled at two relative densities: 20% and 47%. The relative density is calculated as the ratio of the foam density and the fully consolidated aluminum density of 2.7 g/cc. The foam network was constructed by weaving 0.5 mm diameter aluminum strands into a loose network structure with approximately 10 pores per 2.54 cm at an initial relative density near 8%. This structure is then quasi-statically compacted in order to achieve the desired pre-test density. The 47% dense foam structure was scanned using a digital x-ray computed tomography (XCT) system manufactured by NorthStar Imaging (model X50CT), which obtains 1440 two-dimensional images spaced 127 μm apart. The 14-bit grey scale images have a resolution of 947 × 947 pixels and a magnification of 2.5×. The images are stitched together to produce a three-dimensional geometry that was used as initial conditions for the simulations. XCT scans were not available for the 20% foam samples. Instead, the 20% dense foam structures were computationally constructed by punching randomly distributed 100 μm diameter spherical pores into a solid aluminum billet. The pores did not overlap in as much as possible; the resulting foam structure contained the correct pore size distribution and filament characteristic length as compared to the test articles. Images of the computational domains are presented in Figure 2, both a cross-section of the foam structures as well as a three-dimensional illustration of the test configuration. Experiments on 20% dense foam utilized a 1 mm copper anvil witness plate whereas experiments on the 47% foam utilized either copper, aluminum or tantalum witness plates near 4 mm thick.

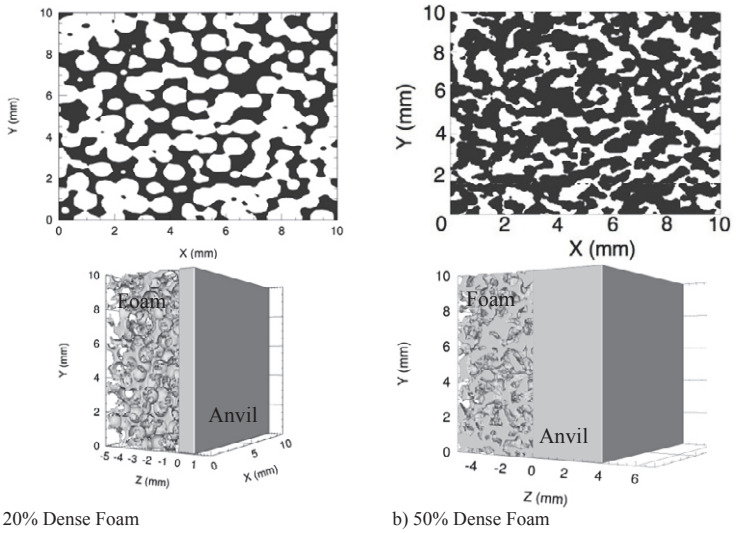

a) 20% Dense Foam b) 50% Dense Foam

Figure 2: Two and three-dimensional illustrations of the computational domain for 20 and 47% foam systems.

The simulations presented here were performed using the Eurlarian hydrocode CTH [8] where periodic boundary conditions were imposed in the lateral direction. A Mie-Grüneisen equation of state (EOS) was used to model both the aluminum foam and witness plate, whereas a sesame EOS was used for the Teflon [9-12]. Figure 3 presents the Teflon temperature-pressure phase space utilized in these simulations. This figure includes the solid crystalline phase (I,II,III) as well as the melt, decomposition and several release isentropes for reference. In low-pressure static experiments, Teflon thermal degradation and melt is initiated near 500 K and melt is complete near 750 K, complete decomposition to carbon and gaseous fluorocarbons occurs at 1000 K [9,11]. The melt and decomposition temperatures increase as pressure increases; see the insert in Figure 3. For shock loaded dynamic experiments melting along the Hugoniot occurs near 1000 K and decomposition near 2000 K (34 GPa) [10,12]. In Figure 3, melt from the low and high-pressure experiments has been connected with an interpolated dotted line. The isentropic release lines are presented in Figure 3 and illustrate how Teflon can decompose and melt upon release. Thus a material shocked to 15 GPa should melt upon release, as illustrated. The thermodynamic melt response of Teflon has been incorporated into a tabular (sesame) equation of state and the decomposition is incorporated via an Arrhenius reaction model that switches between a solid and vapor equations of state [10].

The temperature and strain rate dependent Johnson-Cook visco-plastic model was used to model the strength of the aluminum and Teflon constituents individually [13]. It was found that in order to approximate the VISAR data the strength of the Teflon needed to be set to near zero. The fracture strength (i.e. spall strength) of the aluminum buffer plate was estimated from spall data presented in multiple sources [14,15]. The material parameters used for these constitutive relations are presented on Table 1.

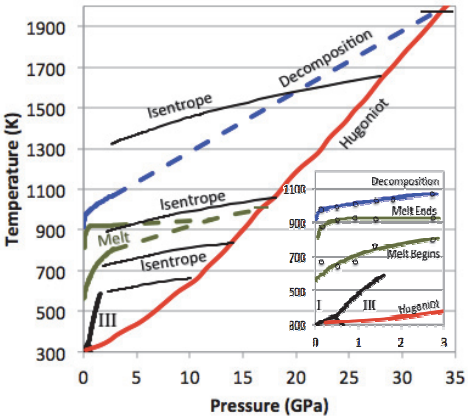

Figure 3: Phase diagram for Teflon. Insert was obtained from static data [11,12]. Shock and release states were calculated from tabular equation of state [10,11,12].

Baseline material and constitutive constants for the mesoscale simulations

Parameter	Aluminium	Parameter	Aluminium
Density, ρ [g/cm^3]	2.703	Strain Coefficient†, A [*GPa*]	0.26496
Zero stress shock speed, C_0 [*km/s*]	5.22	Strain Coefficient†, B [*GPa*]	0.42642
Hugoniot slope, s	1.37	Strain Rate Coefficient†, C	1.5×10^{-2}
Grüneisen coefficient, $\Gamma=V(\partial P/\partial E)_V$	1.97	Thermal exponent†, m	1.0
Specific heat, C_V [*J/(g-K)*]	0.862	Strain exponent†, n	0.34
Fracture strength, σ_s [*GPa*]	0.31	Poisson's ratio, ν	0.33

† Johnson-Cook visco-plastic model constants

In previous high strain rate, $>10^6$ s^{-1}, studies conducted by the authors it has been found that mesh convergence is achieved for 10 computational cells per material element in a given spatial direction. In this study, where the strain rates are lower, the mesh was such that 20 cells per foam filament were needed. Given these requirements and the three-dimensional nature of the domain, the simulations required significant computational resources.

4. Results

4.1. Bulk Response of 47% Aluminum Foam

Figure 4a presents time traces of particle velocity comparing the three-dimensional mesoscale simulations and experimentally obtained VISAR data [1]. Time zero indicates impact of the foam against the stationary witness plate. The 499, 958 and 1435 m/s shots were against an aluminum witness plate whereas the 1983 m/s (not shown) was against tantalum and the 2223 m/s (not shown) was against copper. The mesoscale simulations tend to over predict the experimental data, this over-prediction is increased as impact velocity is increased. In most of the traces presented the various release states, u_i, are maintained for nearly a microsecond, represented by a horizontal dashed line, before reverberating to the next particle velocity state. Both the experimental and simulated particle velocity data demonstrates high frequency oscillations about the average state.

As illustrated in Figure 1, the particle velocity states, u_i, can be converted to a series of average pressure-density states using impedance matching techniques along with the Rankine-Hugoniot jump conditions [1]. The experimental and simulated shock states presented in Figure 4a have been converted to pressure density states and presented in Figure 4b. The filled data points represent the experimental results and the open data points represent the simulated results. The shock Hugoniot fit based on a linear U_s-u_p relation has been presented as solid lines for comparison; the mesoscale simulations are in black whereas the experimental data is in dark grey. One can note the relatively large scatter in the data compared to the mean Hugoniot. Both the two and three-dimensional simulations under-predict the bulk response of the foam, the two-dimensional simulations to a greater degree than the three-dimensional simulations. Given the relatively large porosity of this system, the two-dimensional unfilled foam structures lack the bulk strength obtained from out of plane material

connectivity. The results that follow focus only on three-dimensional simulations; variations resulting from two versus three-dimensional mesoscale simulations requires further investigation [16].

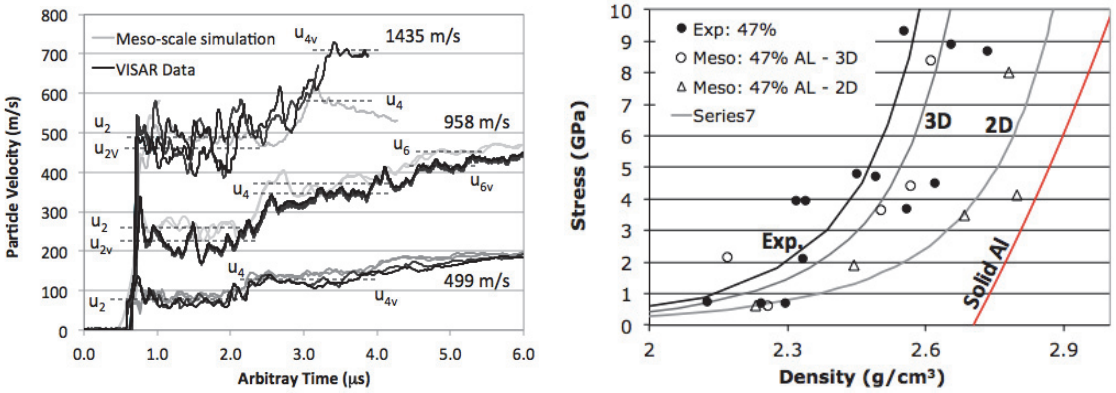

a) Simulated and measured particle velocity response

b) Simulate and measured Hugoniot response

Figure 4: Comparison of measured and simulated response of 47% foam systems.

4.2. Bulk Response of 47% and 20% Aluminum Foam with Teflon Fill

Figure 5a presents the particle velocity obtained from mesoscale simulations for Teflon filled 47% dense aluminum foam. The 499 m/s, 958 m/s and 1435 m/s impact velocities, shown in grey, were against a 4 mm thick aluminum witness plate, whereas the 1983 m/s impact velocity, shown in black, was against a 4 mm thick tantalum witness plate. The arrival time of the stress wave from the 1983 m/s shot is delay as compared to the shots against an aluminum target given the lower wave speed of tantalum compared to aluminum. It also experiences a decrease in the particle velocity starting near 2.5 μs. This decrease results from release wave interactions with the back surface of the foam system and possibly phase change within the Teflon. Figure 5b presents the particle velocity simulations for the 20% aluminum foam systems with Teflon fill against 1 mm thick aluminum witness plates. The shock and release states are clearly visible in these figures.

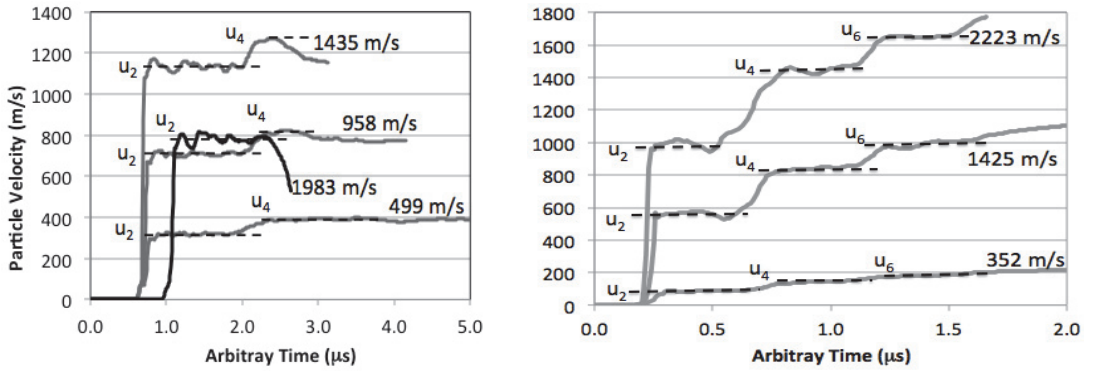

a) 47% Aluminum foam with Teflon fill

a) 20% Aluminum foam with Teflon fill

Figure 5: Simulated response of Teflon filled aluminum foam systems.

Figure 6 presents the bulk pressure-density response of the aluminum Teflon systems presented in Figures 4 and 5. The fully consolidated aluminum and Teflon Hugoniots have been presented for comparison. The unfilled 47% aluminum foam has the softest response; filling the aluminum foam with Teflon results in a stiffer system. Increasing the percent of aluminum increases the stiffness of the system. The bulk response of the mixed aluminum-Teflon systems is between the aluminum and Teflon Hugoniots respectively.

4.3. Hugoniot State Stress Distributions

Although the data presented in Figure 6 represents the average states obtained in the heterogeneous system, the material actually experiences a distribution of states. In order to quantify this distribution, the longitudinal stress of each computational cell, at any instant in time, within the foam was recorded, which translates into approximately 500,000 occurrences of stress given the computational mesh resolution. Figure 7 presents the distribution of stress about the Hugoniot state for a single snapshot in time for the various impact velocities; the average stress states have been indicated with a dashed line. The amplitude of the data is presented as *Fractional Occurrence*, which appears to be quite small. The amplitudes are misleading given the small bin size selected and that the initial shock has not completely traversed the foam resulting in quite a few occurrences of zero stress. Thus one should focus on the shape of the distribution and not the amplitude.

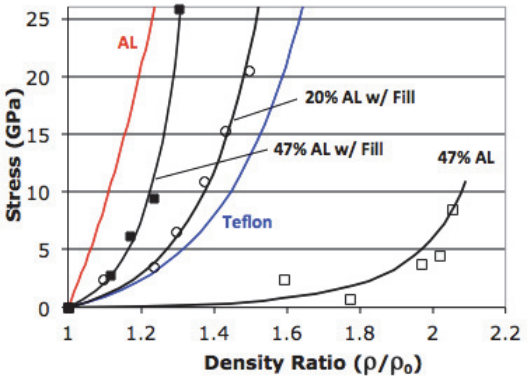

Figure 6: Hugoniot state comparison of bulk mesoscale simulation with and without Teflon fill.

Figure 7a presents the stress distributions of the 47% dense aluminum foam whereas Figure 7b presents the stress distributions of the 47% dense aluminum-Teflon system. The distributions for the filled systems are much smoother than the unfilled systems. The shape of the distribution, especially at high stress levels, is of interest given the possibility of melt and/or disassociation of the Teflon near 30 GPa. At the highest stress levels achieved (at impact velocities near 1983 m/s against the tantalum anvil), the average stress induced in the Teflon is near 20 GPa, with significant occurrences as high as 30 GPa. Within the framework of the simulations, Teflon is modeled with a sesame look-up table equation of state, where degradation is modeled as a change in phase in the material triggered at 30 GPa. Initial inspection of the data yields little to no melt or decomposition in the shocked state. Further investigation of the data is necessary in order to assess the extent of reaction within these systems.

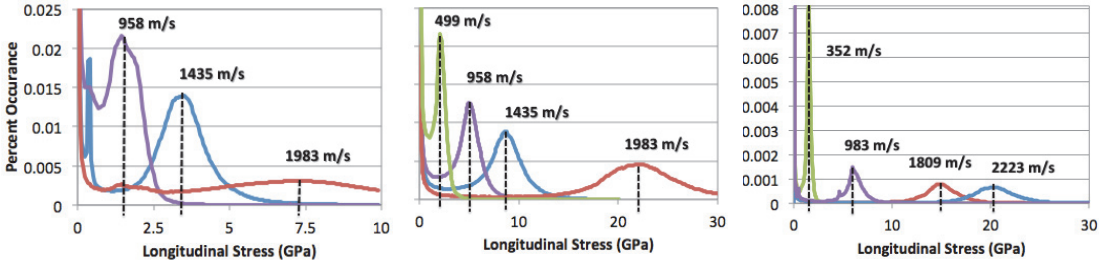

a) 47% Al Foam unfilled

b) 47% Al Foam with Teflon

c) 20% Al Foam with Teflon

Figure 7: Stress distributions in aluminum and aluminum Teflon systems over a range of impact velocities.

4.4. Time Variations of Stress Distributions

Figure 8 presents stress distributions in the foam systems for a specific impact velocity at various instances in time, as indicated within the figures. Over the time window presented, the systems experience both loading (shock) and unloading

(release) states. In early time, the stress distribution is centered about the Hugoniot stress presented in Figure 7. However as time progresses the unloading stress distributions differ depending on the composition of the system. For the unfilled 47% aluminum foam presented in Figure 8a, the occurrence of Hugoniot stress centered about the average stress of 7 GPa decreases and gives rise to various lower stress states of release. In general this process of unloading occurs as a smooth exchange of modes: a decrease in the amplitude of stress occurrence centered about the Hugoniot stress to successive release states. Thus as time progresses there appears a single mode of stress that is characteristic of the system's response for any given instant in time. This is in contrast to the 47% aluminum-Teflon filled systems (Figure 8b) in which an entire range of stress states, from the Hugoniot stress down to zero, emerges as time passes. Release processes decay the higher stress states while a lower release stress state emerges; all the while, there are significant occurrences of stress down to zero. Thus, the presence of the fill not only decreases the time it takes this release process to occur, i.e. increases the wave speeds within the system, but also supports a large multivalued distribution of stress states within the system. Figure 8c presents the time evolution of the shock and release process for the 20% aluminum-Teflon system. As the percent of aluminum is reduced from 47% to 20%, while the percent Teflon is increased, the single mode response seen in the porous aluminum foam re-emerges. The stress distributions indicate a system characterized by an exchange of modes as the system shocks and then releases within the microstructure itself. We might speculate that this results from a single material dominating the response of the overall material. Thus one would conclude that a requirement of broadband distributions in stress, presented in Figure 8b, is significant percentages of multiple materials. The shape of the stress distribution as the system undergoes release is largely affected by the percent mix of aluminum and Teflon. The exact mechanism governing the release behavior in the 47% versus 20% aluminum Teflon filled foam systems is still under investigation.

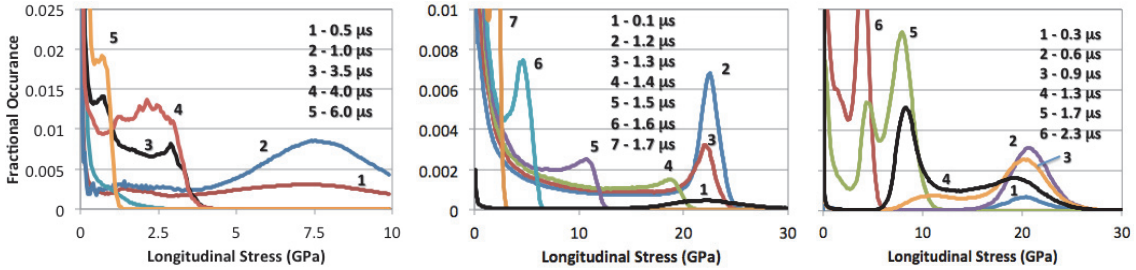

a) 47% Al Foam, 1983 m/s

b) 47% Al Foam Teflon filled, 1983 m/s

c) 20% Al Foam filled, 2223 m/s

Figure 8: Shifting stress distributions as foam undergoes shock and release processes at specific impact velocities.

4.5. Hugoniot State Temperature Distributions

It should be noted that CTH assumes pressure equilibrium within each computational cell. Thus mixed materials within a cell must have the same pressure. Although the pressure within a cell is constant, the temperature is not. Thus the aluminum and Teflon can achieve different temperatures within a given cell. The result is a different temperature distribution for each material as compared to a single stress distribution for the system. Figure 9 presents the aluminum and Teflon temperature distribution after the initial compaction wave has passed. The results indicate that the Teflon experiences significantly higher average temperature, 670 K, as compared to the aluminum, near 400 K. It is also interesting to note that the Teflon experiences non-zero occurrences in temperature, near 1,000 K, as a result of the heterogeneous loading, i.e. temperatures near the onset of melt. Thus even at relatively low impact velocities the temperature within the heterogeneous system can experience significant deviations from the mean. These deviations can give rise to material response such as melt and decomposition, can significantly increase the irreversibility of the material's response and increase entropy production. Mechanisms, which give rise to these high temperature hot spots, include localized shear and impedance mismatch; hot spots have been well documented in the literature.

4.6. Isentropic Release

In order to further characterize the dynamic response of the aluminum foam systems, the isentropic release states were calculated from both the experimental data and mesoscale simulations. Release data was calculated by impedance matching the release states obtained from the VISAR traces, see Figure 1b; an identical procedure was followed for the simulated data. In addition, an analytic isentrope was constructed for the aluminum foam systems by combining the 2nd law of thermodynamics, $dE=Tds-PdV$ and the Mie-Grüneisen equation of state. More details of this process can be found in Asay

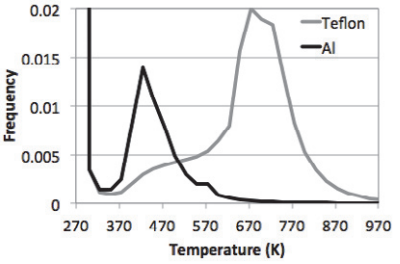

Figure 9: Temperature distributions in 20%-Aluminum and 80%-Teflon resulting from an impact at 1425 m/s at 0.3 μs.

[2], who developed isentropes for unfilled 60% dense porous aluminum systems. The combined equation yields the following ordinary differential equation (ODE) which describes the hydrostatic isentropic pressure (longitudinal stress), P, as a function of specific volume, V:

$$\left(\frac{\partial P}{\partial V}\right)_s = \left(\frac{dP_r}{dV}\right)\left(1-\gamma_0\left(1-V/V_0\right)/2\right)+\frac{\gamma_0}{2V_{0s}}P_r-\frac{\gamma_0}{V_{0s}}P \tag{1}$$

where P_r is the reference curve, γ_0 is the Grüneisen parameter, V_0 and V_{0s} are the initial specific volumes of the heterogeneous system and the solid material respectively. The particle velocity, u, during release can be calculated from the Riemann integral:

$$u-u_i=-\int_{V_i}^{V}\left[\left(-\frac{\partial P}{\partial V}\right)_s\right]^{1/2}dV \tag{2}$$

These equations, which describe the release isentrope, were integrated from the Hugoniot state to zero pressure using a Rung-Kutta scheme, as outlined by Asay [2]. The results are presented in Figure 9.

Figure 10a presents the results for the 47% aluminum foam system in stress-particle velocity space, at various impact velocities along with the data from Asay for comparison. The solid black line is the Hugoniot while the color lines are the analytic release isentropes. The solid points are experimental data whereas open points are simulated data. At low initial pressures the release isentrope passes reasonably near both the experimental and simulated release points. However, as the impact velocity is increased and the Hugoniot stress rises, the analytic isentrope deviates significantly from the experimental and simulated data. Both the data and experiment suggest there are more irreversibilites than those represented by the analytic release isentrope. These irreversibilites could be a result of melt, degradation and decomposition of the Teflon. The data of Asay, although at higher initial density as compared to the aluminum foam investigated here, is well represented by the analytic release isentrope.

Figures 10b and 10c present the simulated data for the 20% aluminum Teflon filled system. The shock Hugoniot for the aluminum-Teflon system is represented by the solid black line and is bound between the consolidated aluminum and Teflon Hugoniots. The simulated shock states are presented as open circles followed by the release isentropes presented colored lines. Unlike the 47% unfilled foam, the isentropic release of the 20% aluminum Teflon systems appear to follow the shock Hugoniot more closely. An interesting feature of the release behavior is the change in slope of the isentrope in stress velocity space near 5 GPa. This same change in slope is not as obvious in stress density ratio space.

5. Conclusions

Reverse ballistic experiments have been conducted on aluminum foam systems at 47% initial density. The simulations presented in this work focus on initially modeling the experimental results and then go on the make predictions of mixed aluminum-Teflon systems at 47 and 20% initial aluminum foam density. The advantage to mesoscale modeling is its ability to *predict* the dynamic response in the absence of experimental data, for a variety of constituent mixtures. Since pore collapse is modeled explicitly, no experimental data is needed to drive the simulations.

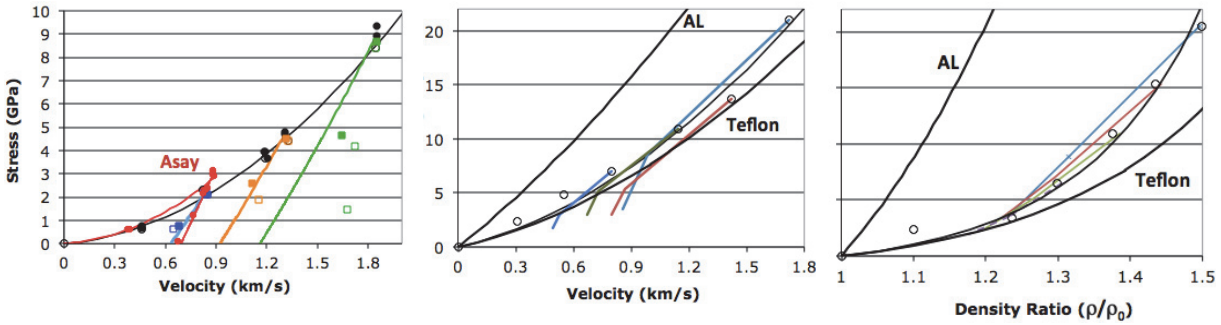

a) 47% Al Foam b) 20% Al Foam with Teflon Fill c) 20% Al Foam with Teflon Fill

Figure 10: Shock and release data. a) 47% Al foam, solid colored lines represents analytic release curves, solid points are experimental data and open points are simulated data b) and c) 20 % Al with Teflon simulated data, solid black lines are shock Hugoniots and color lines are release isentropes.

These simulations give us some insight into how the mixed materials behave under dynamic loading and unloading processes. As the relative percent of Teflon is increased, the dynamic bulk response of the system tends to follow the Hugoniot response of the fully consolidated Teflon. The stress and temperature distributions give us initial threshold conditions in which melt and thermal degradation might initiate. Ultimately this includes providing functionality with respect to constituent mix and impact velocity leading to complete phase change.

The simulated Hugoniot state achieved in the 47% dense foam match the experimental data well. In addition, simulated release from low Hugoniot stresses matches the available data. As the Hugoniot stress is increased above 5 GPa, the release states predicted from the simulations deviate more from the experimental data. However, they do appear to be relatively closer than homogeneous analytic prediction utilizing a Mie-Grüneisen equation of state. The experimental data suggests that there is significantly more irreversible behavior during release than predicted by the analytic solution, possibly due to melt and thermal degradation. Further investigation into the sources of these irreversibilities is needed in order to improve future capabilities.

The simulated Hugoniot states achieved in the 20% aluminum foam-Teflon systems tends to closely follow the fully consolidated Teflon Hugoniot. The release behavior of the mixed foam-Teflon systems is more complicated. The release isentropes initially tend to follow the Teflon Hugoniot until they reach the intersection of the fully consolidated aluminum and Teflon Hugoniots (near 5 GPa) at which point the release isentropes slope changes. The dynamic response, specifically during release, needs to be explored further to understand the relative interactions of the binary system.

Unlike experiments, the mesoscale simulations yield a distribution of mechanical and thermodynamic states, which can be important when assessing the effects of melt, material decomposition and possibly reaction. These distributions in state are a direct consequence of the heterogeneous nature of the material. The anisotropic states vary not only as a function of spatial location with in the material but also as a function of time as local shock and release processes occur. Thus mesoscale simulations are a step forward in our ability to assess and predict the complicated interactions of dynamically loaded heterogeneous systems.

X-ray computed tomography (XCT) scans for the 20% foam are planned. We plan to repeat the simulations presented here using actual geometries obtained from foam samples. In so doing we can assess the sensitivity of our results while using actual versus computationally constructed geometries. In addition reverse ballistic experiments on 20% aluminum foam with a fluoropolymer fill are planned. We plan to compare the response of the 20% aluminum Teflon filled systems results presented here to experimental data. In so doing we can further assess the capabilities and deficiencies of mesoscale simulations.

Acknowledgements

This work was completed with funding support provided by the Air Force Research Laboratory under contract F1TBAX9111B701.

References

[1] Maines, W.R., Borg, J.P., Reinhart, W.D., Neel, C., Nixon, M. and Chhabildas, L. C., Release States In Aluminum Foam, APS-*Shock Compression of Condensed Matter*, AIP Conf. Proc. 1426, pg 1439-42 (2012)
[2] Asay, J.R. Shock and release behavior in Porous 1100 Aluminum, *Journal of Applied Physics* 46, 197, 1975.
[3] B. M. Butcher, M. M. Carroll, and A. C. Holt, Shockwave compaction of porous aluminum, *Journal of Applied Physics* 45, 3864
[4] Bonnan, S., Hereil, P. L. and Collombet, F. Experimental characterization of quasi static and shock wave behavior of porous aluminum *Journal of Applied Physics* 83, 5741 1998.

[5] Linde, R.K. and Schmidt, D.N., Shock propagation in Nonreactive porous solids, *Journal of Applied Physics*. 37, 3259, 1966
[6] Richard G. Kraus, R.G., Chapman, D.J., Proud, W.G and Swift, D.C., Hugoniot and spall strength measurements of porous aluminum, *Journal of Applied Physics* 105, 114914, 2009
[7] Harris, E.J., Winter, R., Cotton, M., Swan, M. and Maw, J.R. Measurements of the shock response of porous structures formed by selective laser melting APS-*Shock Compression of Condensed Matter,* AIP Conf. Proc. 1426, pg 1431-34 (2012)
[8] McGlaun, J. M. Thompson, S. L. and Elrick, M. G., "CTH: a Three-Dimensional Shock Wave Physics Code," *Int. J. Impact Engng.*, **10**, 351-360, 1990.
[9] Rice, MH, McQueen, R.G. and Walsh, J.M. "Compression of Solids by Strong Shock Waves" *Solid State Phys*. 6 (1), 1958.
[10] Kerley, G.I. A reactive equation of state model for Teflon. NSWCDD/TR-00/78, 1996
[11] Tamayama, M.; Andersen, T. N.; and Eyring, H., "The Melting and Pyrolysis of Teflon and the Melting of Silver Chloride and Iodine Under High Pressure," Proc. Natl. Acad. Sci., Vol. 57, 1967, pp. 554-561.
[12] Morris, C. E.; Fritz, J. N.; and McQueen, R. G., "The Equation of State of Polytetrafluoroethylene to 80 GPa," J. Chem. Phys., Vol. 80, 1984, pp. 5203-5218.
[13] Johnson, G. R. and Cook, W. H., 1985. Fracture characteristics of three metals subjected to various strains, strain rates, temperatures and pressures. Engineering Fracture Mechanics 21, 31-48.
[14] Moshe, E., Eliezer, S., Dekel, E., Ludmirsky, A., Henis, Z., Werdiger, M., Goldberg, I.B., 1998. An increase of the spall strength in aluminium, copper, and Metglas at strain rates larger than 10^7 s^{-1}. Journal of Applied Physics 83, 4004–4011.
[15] Davison, L., Graham, R.A., 1979. Shock Compression of Solids. Physics Reports 55, 255–379.
[16] Borg, J.P. and Vogler, T.J. Rapid Compaction of Granular Material: Characterizing Two and Three-Dimensional Mesoscale Simulations, Shock Waves (under review)